Instabilities of concentration stripe patterns in ferrocolloids

A. Cēbers
Institute of Physics, University of Latvia, Salaspils-1, LV-2169, Latvia
(Received 10 May 1999)

Equations describing the kinetics of the phase separation in ferrocolloids in a Hele-Shaw cell under the action of a rotating magnetic field are proposed. Numerical simulation on the basis of a pseudospectral technique demonstrates that upon the action of a rotating field on a magnetic colloid which undergoes the phase separation a periodical system of stripes parallel to the plane of a rotating magnetic field stripes is created. The period of a structure found numerically satisfactorily corresponds to the one calculated on the basis of the energy minimum. Thus, the undulation instability leading to the formation of chevron structures takes place if the tangential component of a rotating magnetic field is eliminated, whereas the normal component is increased at the same time. If during the development of the undulation deformations of a concentration pattern the magnetic Bond number is large enough the secondary instabilities may occur leading to the fingering of stripes to bring about merging and break-up of stripes. It is shown that an increase in the magnetic Bond number leads to the onset of the instability at the boundaries between the regions with homogeneous orientation of stripes as well as to formation of the characteristic hairpin patterns.

PACS number(s): 47.54.+r, 75.50.Mm

I. INTRODUCTION

The magnetic-field-induced phase separation in magnetic fluids has received extensive attention during the last years [1–10]. The resulting patterns are determined by the competition between the self-magnetic field energy of a structure and the surface energy of the phase boundaries [11–13] in the way similar to the formation of a domain structure in ferromagnetics [14]. As to the patterns resulting upon the magnetic-field-induced phase separation in thin layers the hexagonal and stripe structures may form depending on the physical parameters of a system [15,16]. At the concentration values near the critical point a stripe pattern is energetically more advantageous [16]. Since there is no preferred direction along the boundaries of a layer the stripe pattern usually takes the shape of a labyrinth. It is possible to generate a system of directionally ordered stripes or 2D magnetic smectics by applying a tangential magnetic field to the layer. Now, upon increasing the magnetic-field strength which is applied normally to the boundaries of a layer upon the said 2D magnetic smectics one can observe formation of the chevron structure [17]. It is shown by numerical simulation that by applying high-frequency rotating magnetic fields it is possible to obtain a regular periodic system of the magnetic stripes the period of which diminishes with an increase in the field strength. Thus, the elimination of the tangential component of a rotating field alongside with a simultaneous increase in the normal component allows to induce the undulation instability of a parallel system of magnetic stripes. In order to demonstrate this the numerical simulation is carried out on the basis of equations of the Cahn-Hilliard model for kinetics of the phase transformations [18] which are generalized to account for the long-range magnetic forces [19–21]. Such equations corresponding to the case of a planar layer of a magnetic colloid upon the action of a normal field are proposed in Refs. [21,22]. The novelty proposed here consists in adding a term to the said equations to describe the action of a component of a rotating magnetic field which is tangentially oriented with respect to the boundaries of a plane layer.

II. KINETICS OF THE PHASE SEPARATION IN A ROTATING MAGNETIC FIELD

Let us consider a magnetic colloid in a plane layer upon the action of a magnetic field, which rotates in the plane normal to the layer. Let us calculate the part of the variation of the thermodynamic potential of the system up to the second order terms resulting upon the concentration perturbation δn. Equations for the magnetic field perturbation $\delta \boldsymbol{H}$ (neglecting the anisotropy of the magnetic susceptibility χ) follow

$$\mathrm{div}\left(\delta \boldsymbol{H} + 4\pi\chi \delta \boldsymbol{H} + 4\pi \frac{\partial \boldsymbol{M}}{\partial n} \delta n \right) = 0$$

$$\mathrm{rot}(\delta \boldsymbol{H}) = \boldsymbol{0}, \tag{1}$$

where the boundary conditions on the surfaces of a layer $z = \pm h/2$ with the external normal $\boldsymbol{\nu}$ read

$$\mu \boldsymbol{\nu} \cdot \delta \boldsymbol{H}^i + 4\pi \frac{\partial \boldsymbol{M}}{\partial n} \cdot \boldsymbol{\nu} \delta n = \boldsymbol{\nu} \cdot \delta \boldsymbol{H}^e,$$

$$\delta \boldsymbol{H}_t^i = \delta \boldsymbol{H}_t^e . \tag{2}$$

Upon introduction of the potential of a perturbed magnetic field according to $\delta \boldsymbol{H} = \boldsymbol{\nabla} \delta\psi$ the variation of the thermodynamic potential up to the terms of the second order yields $[(\delta \boldsymbol{M})_n = (\partial \boldsymbol{M}/\partial n)\delta n]$

$$\Delta F = -\int \boldsymbol{M}\cdot\delta\boldsymbol{H}dV - \frac{1}{2}\chi\int (\delta\boldsymbol{H})^2 dV - \int (\delta\boldsymbol{M})_n\cdot\delta\boldsymbol{H}dV$$
$$-\frac{1}{4\pi}\int \boldsymbol{H}\cdot\delta\boldsymbol{H}dV - \frac{1}{8\pi}\int (\delta\boldsymbol{H})^2 dV$$
$$= \frac{1}{8\pi}\int \mu(\delta\boldsymbol{H})^2 dV. \quad (3)$$

Let us consider the energy of the perturbed magnetic field of a structure defined in Eq. (3) by letting $\mu=1$ to account for the energy of the self-magnetic field of a system in the first nonvanishing approximation. Thus, in accordance with the equation and the boundary conditions for the magnetostatic potential

$$\Delta\,\delta\psi^i = -\frac{4\pi}{\mu}\frac{\partial\boldsymbol{M}}{\partial n}\cdot\boldsymbol{\nabla}\,\delta n, \quad (4)$$

$$\delta\psi^i = \delta\psi^e;\quad \frac{\partial\,\delta\psi^e}{\partial\nu} - \mu\frac{\partial\,\delta\psi^i}{\partial\nu} = 4\pi\frac{\partial\boldsymbol{M}}{\partial n}\cdot\boldsymbol{\nu}\delta n \quad (5)$$

we arrive at the following expression

$$\delta\psi(\boldsymbol{\rho},z) = \int \frac{(\partial\boldsymbol{M}/\partial n)\cdot\boldsymbol{\nabla}\,\delta n}{\sqrt{(\boldsymbol{\rho}-\boldsymbol{\rho}')^2+(z-z')^2}}dV'$$
$$-\int \frac{(\partial\boldsymbol{M}/\partial n)\cdot\delta n\,\boldsymbol{\nu}}{\sqrt{(\boldsymbol{\rho}-\boldsymbol{\rho}')^2+(z-z')^2}}dS'. \quad (6)$$

Let us consider the processes of pattern formation in the assumption that the concentration remains constant across the layer. Although the processes leading to formation of the multilayer structures can not be ruled out [23] even this approximation yields a system with a versatile patterning opportunities. Subsequently, the energy of the self-magnetic field transforms into

$$\Delta F = -\frac{1}{2}\int \frac{\partial\boldsymbol{M}}{\partial n}\cdot\boldsymbol{\nu}\delta\psi dS + \frac{1}{2}\int \delta\psi\frac{\partial\boldsymbol{M}}{\partial n}\cdot\boldsymbol{\nabla}\,\delta n dV. \quad (7)$$

When the period of a field is much smaller than the characteristic time of relaxation of the concentration distribution it is possible to average relation (7) with the respect to the direction of a rotating field. Since the concentration gradient is parallel to the boundaries of a layer the two terms in relation (6) describing the magnetostatic potential give independent contributions to the energy functional. The resulting contribution to the energy functional due to the long-range magnetic interactions equals

$$\Delta F_m = \frac{1}{2}\left(\frac{\partial M}{\partial n}\right)^2\Bigg[\int dS\int dS'\,\delta n(\boldsymbol{\rho})\,\delta n(\boldsymbol{\rho}')$$
$$\times\left(\frac{1}{\sqrt{(\boldsymbol{\rho}-\boldsymbol{\rho}')^2}} - \frac{1}{\sqrt{(\boldsymbol{\rho}-\boldsymbol{\rho}')^2+h^2}}\right)$$
$$+\frac{1}{2}\int dS\int dS'\,\boldsymbol{h}_0\cdot\boldsymbol{\nabla}\,\delta n(\boldsymbol{\rho})\,\boldsymbol{h}_0\cdot\boldsymbol{\nabla}\,\delta n(\boldsymbol{\rho}')$$
$$\times\int_{-h/2}^{h/2}dz\int_{-h/2}^{h/2}dz'\frac{1}{\sqrt{(\boldsymbol{\rho}-\boldsymbol{\rho}')^2+(z-z')^2}}\Bigg] \quad (8)$$

where $\boldsymbol{h}_0$ is the unit vector in the plane of a rotating field along the boundary of a plane layer. Expression (8) defines the contribution to the energy functional of the long-range magnetic interactions in a high-frequency rotating field . Another part of the thermodynamical potential for the states near the critical point takes the traditional form [18,19]

$$\Delta F = -\tfrac{1}{2}\int \alpha(\delta n)^2 dV + \tfrac{1}{4}\int \gamma(\delta n)^4 dV + \tfrac{1}{2}\int \beta(\nabla\,\delta n)^2 dV. \quad (9)$$

When the phase separation is induced by an external field the following expressions for the coefficients α and γ are valid $\alpha=(\partial^2 M/\partial n^2)(H-H_c)$; $\gamma=\frac{1}{6}(\partial^3\varphi/\partial n^3)(n_c,T,H_c)$ [21], where φ is the chemical potential of the particles, n_c and H_c are the concentration and the field strength corresponding to the critical point; $\alpha>0$ if $H>H_c$. The third term in relation (8) is responsible for the surface energy of emerging interphase boundaries. The particle conservation law gives

$$h\frac{\partial\,\delta n}{\partial t} = -\,\mathrm{div}(\boldsymbol{J}),$$

where the expression for the diffusion flux of the particles can be obtained from the following relation:

$$\frac{dS_{\mathrm{tot}}}{dt} = -\frac{1}{T}\frac{d(\Delta F+\Delta F_m)}{dt}$$
$$= -\frac{1}{T}\int \boldsymbol{J}\cdot\boldsymbol{\nabla}\Bigg\{-\alpha\,\delta n+\gamma\,\delta n^3$$
$$-\beta\Delta\,\delta n - \frac{1}{2}\left(\frac{\partial M}{\partial n}\right)^2\frac{1}{h}\mathrm{div}\Bigg[\boldsymbol{h}_0\int T(\boldsymbol{\rho}-\boldsymbol{\rho}')$$
$$\times(\boldsymbol{h}_0\cdot\boldsymbol{\nabla})\,\delta n(\boldsymbol{\rho})dS'\Bigg] + \frac{1}{2}\left(\frac{\partial M}{\partial n}\right)^2\frac{2}{h}$$
$$\times\int J(\boldsymbol{\rho}-\boldsymbol{\rho}')\,\delta n(\boldsymbol{\rho}')dS'\Bigg\}dS$$

in accordance with the linear law in the thermodynamics of the irreversible processes

$$\boldsymbol{J} = -\frac{hn_c}{\delta}\boldsymbol{\nabla}\Bigg\{-\alpha\,\delta n+\gamma\,\delta n^3-\beta\Delta\,\delta n+\frac{1}{2}\left(\frac{\partial M}{\partial n}\right)^2\frac{2}{h}$$
$$\times\int J(\boldsymbol{\rho}-\boldsymbol{\rho}')\,\delta n(\boldsymbol{\rho}')dS' - \frac{1}{2}\left(\frac{\partial M}{\partial n}\right)^2\frac{1}{h}\mathrm{div}$$
$$\times\Bigg[\boldsymbol{h}_0\int T(\boldsymbol{\rho}-\boldsymbol{\rho}')(\boldsymbol{h}_0\cdot\boldsymbol{\nabla})\,\delta n(\boldsymbol{\rho}')dS'\Bigg]\Bigg\} \quad (10)$$

the function $T(\boldsymbol{\rho},h)$ is defined by the following relation:

$$T(\boldsymbol{\rho},h) = \int_{-h/2}^{h/2}\int_{-h/2}^{h/2}dz\,dz'\frac{1}{\sqrt{(\boldsymbol{\rho})^2+(z-z')^2}}$$

and $J(\boldsymbol{\rho},h)$ as

$$J(\boldsymbol{\rho},h) = \frac{1}{\sqrt{\boldsymbol{\rho}^2}} - \frac{1}{\sqrt{\boldsymbol{\rho}^2+h^2}}.$$

The resulting equation for the concentration perturbations takes the following form:

$$\frac{\partial \delta n}{\partial t}=\frac{n_c}{\delta}\Delta\left\{-\alpha\delta n+\gamma\delta n^3-\beta\Delta\delta n+\frac{1}{2}2\left(\frac{\partial M}{\partial n}\right)^2\frac{1}{h}\times\int J(\boldsymbol{\rho}-\boldsymbol{\rho}')\delta n(\boldsymbol{\rho}')dS'-\frac{1}{2}\left(\frac{\partial M}{\partial n}\right)^2\frac{1}{h}\mathrm{div}\times\left[\boldsymbol{h}_0\int T(\boldsymbol{\rho}-\boldsymbol{\rho}')(\boldsymbol{h}_0\cdot\nabla')\delta n(\boldsymbol{\rho}')dS'\right]\right\}. \quad (11)$$

To transform Eq. (11) in an undimensional form the following characteristic scales are to be introduced: the length $\sqrt{\beta/\alpha}$, the time $\delta l^2/n_c\alpha$, the concentration $\sqrt{\alpha/\gamma}$. Thus, upon introduction of the magnetic Bond number $\mathrm{Bm}=(\partial M/\partial n)^2(h/l\alpha)$, Eq. (11) transforms into

$$\frac{\partial\varphi}{\partial t}+\Delta\left\{\varphi-\varphi^3+\Delta\varphi-\frac{\mathrm{Bm}}{\left(\frac{h}{l}\right)^2}\int J(\boldsymbol{\rho}-\boldsymbol{\rho}')\varphi(\boldsymbol{\rho}')dS'+\frac{1}{2}\frac{\mathrm{Bm}}{(h/l)^2}\mathrm{div}\left[\boldsymbol{h}_0\int T(\boldsymbol{\rho}-\boldsymbol{\rho}')(\boldsymbol{h}_0\cdot\boldsymbol{\nabla}')\varphi(\boldsymbol{\rho}')dS'\right]\right\}=0. \quad (12)$$

III. ALGORITHM FOR NUMERICAL SIMULATION

A numerical simulation of the kinetics of the phase transformation described by Eq. (12) is performed using the pseudospectral method [24]. For this purpose the pattern is assumed to be periodic with the periodicity box of dimensions L_x and L_y in x and y directions, respectively. A concentration field is represented by Fourier series

$$\varphi=\sum_{\boldsymbol{q}}\varphi(\boldsymbol{q})\exp(i\boldsymbol{q}\cdot\boldsymbol{\rho}),$$

where $\boldsymbol{q}=(2\pi n_x/L_x,2\pi n_y/L_y)$ (n_x,n_y are integers). A mesh with N_x and N_y points along x and y axis, respectively, is introduced into a periodicity box. The differential operators are approximated by the finite differences. In accordance with Eq. (12) the following equation for the Fourier components of the concentration field is arrived at ($\Delta_x=L_x/N_x$, $\Delta_y=L_y/N_y$ are the mesh sizes in x and y directions, respectively)

$$\frac{d\varphi_{\boldsymbol{q}}}{dt}+\frac{2}{\Delta_x^2}\left\{\cos\left(\frac{2\pi n_x}{N_x}\right)-1+\left(\frac{\Delta_x}{\Delta_y}\right)^2\left[\cos\left(\frac{2\pi n_y}{N_y}\right)-1\right]\right\}\times\left\{\left[1+\frac{2}{\Delta_x^2}\left(\cos\left(\frac{2\pi n_x}{N_x}\right)-1+\left(\frac{\Delta_x}{\Delta_y}\right)^2\times\left[\cos\left(\frac{2\pi n_y}{N_y}\right)-1\right]\right)-\frac{\mathrm{Bm}}{(h/l)^2}\left(\frac{1}{2}\frac{\sin^2(2\pi n_x/N_x)}{\Delta_x^2}T(\boldsymbol{q})-J(\boldsymbol{q})\right)\right]\varphi(\boldsymbol{q})-\varphi^3(\boldsymbol{q})\right\}=0, \quad (13)$$

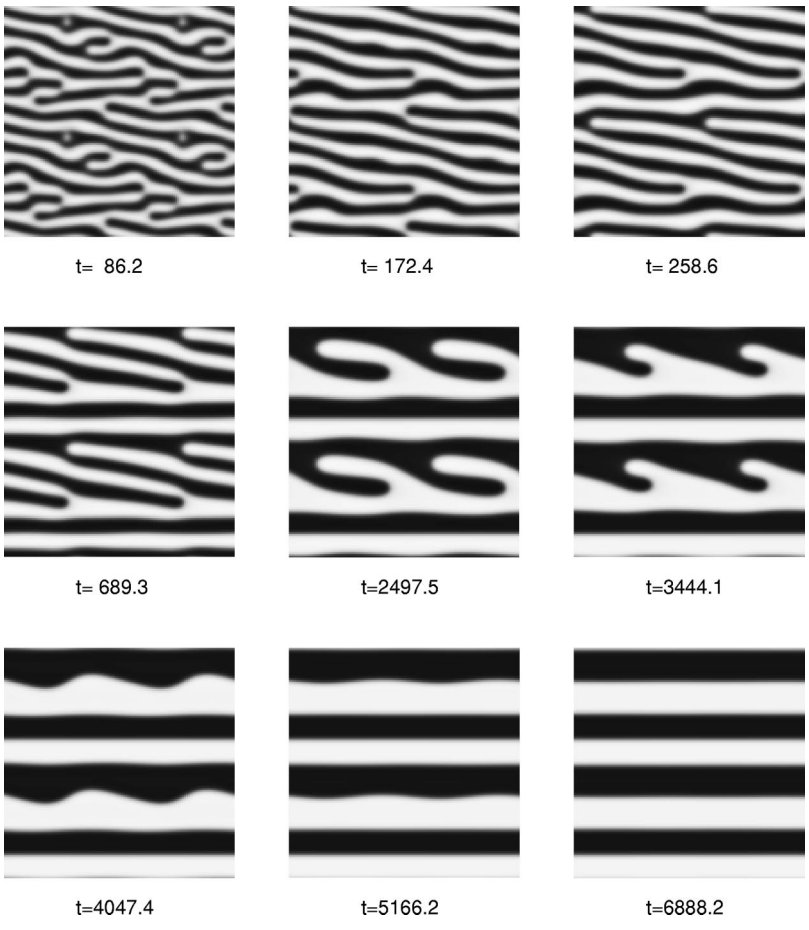

FIG. 1. Structure rearrangement upon the action of the rotating magnetic field. Initial state corresponds to the random perturbation with amplitude $\epsilon=0.01$ around critical concentration. The dark and white designate a positive and negative sign of the concentration perturbation around critical one. Time is given in undimensional units. $h/l=5$. $\mathrm{Bm}=0.2$; mesh size 64×64.

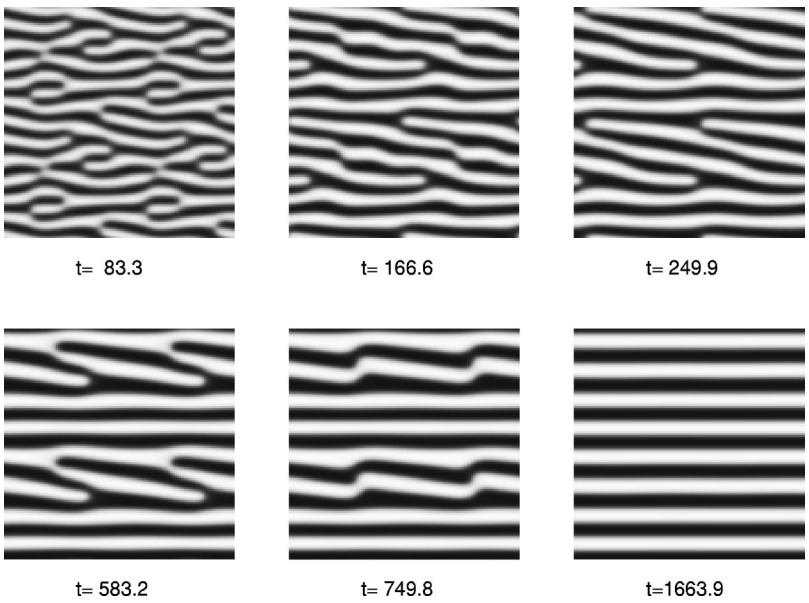

FIG. 2. The same as in Fig. 1, except for Bm=0.4.

where the following expressions are valid for the Fourier transforms of the kernel functions describing the dipolar interactions in the system $T(\boldsymbol{q})$ and $J(\boldsymbol{q})$:

$$T(\boldsymbol{q})=\frac{4\pi}{\|\boldsymbol{q}\|^3}\left[\frac{h}{l}\|\boldsymbol{q}\|-1+\exp\left(-\frac{h\|\boldsymbol{q}\|}{l}\right)\right]$$

$$J(\boldsymbol{q})=2\pi\frac{[1-\exp(-h\|\boldsymbol{q}\|/l)]}{\|\boldsymbol{q}\|}.$$

The Fourier component of the nonlinear term $\varphi^3(\boldsymbol{q})$ is calculated traditionally, i.e., the values of the function at meshpoints are found by employing the inverse Fourier transform, φ^3 at the meshpoints is calculated and, subsequently, $\varphi^3(\boldsymbol{q})$ is found by applying the direct Fourier transform to the calculated results. The temporal evolution described by Eq. (12) under the present case is investigated by the Euler method. Attention must be paid to escape numerical instabilities. In order to avoid numerical instabilities a time step for the Euler schema is applied in accordance with the following relation:

$$\Delta t=\frac{\Delta_x^4}{8\{8+[2\pi(\mathrm{Bm}/(h/l))-1]\Delta_x^2\}}.$$

IV. RESULTS OF NUMERICAL SIMULATION

Equation (12) for formation of the patterns in a rotating magnetic field describes a rather broad class of phenomena. Let us consider kinetics of the stripe formation upon the action of the rotating magnetic field. The nonhomogeneous structures which are formed as a result of spinodal decomposition in accordance with Eq. (12) transform to the stripelike one oriented parallel to the plane of a rotating field. The fourth term under the Laplacian in Eq. (12) is responsible for

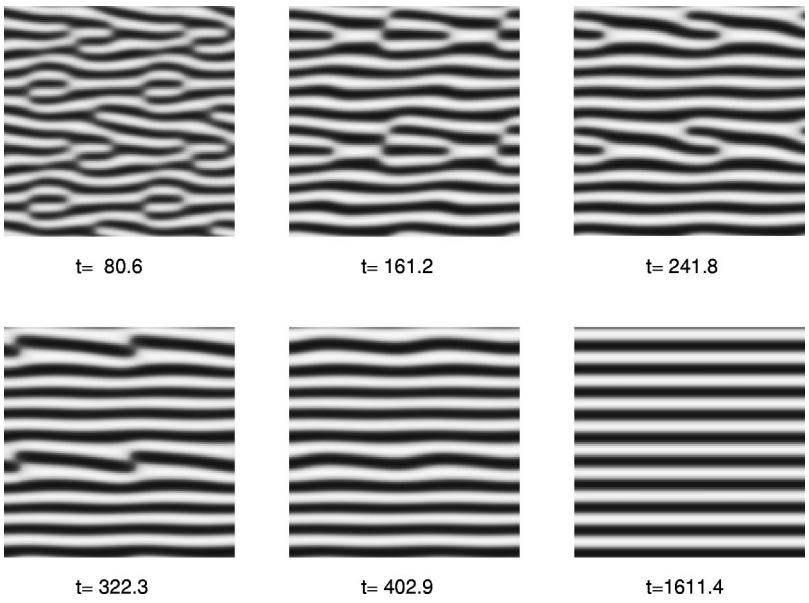

FIG. 3. The same as in Fig. 1, except for Bm=0.6.

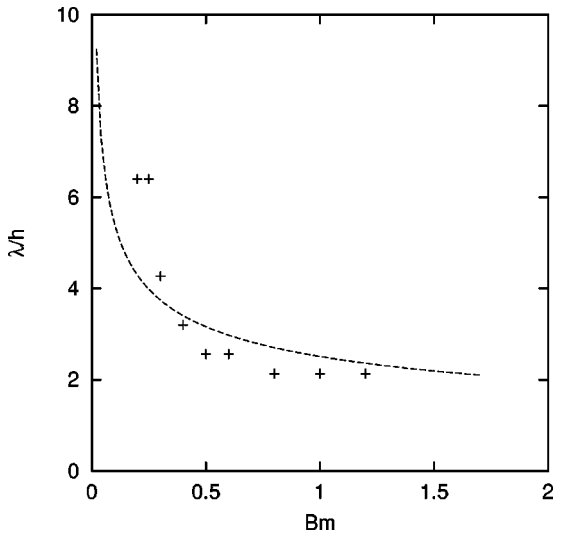

FIG. 4. The dependence of the structure period of a stripe pattern upon the magnetic Bond number. $h/l=5$. The broken line reflects the ratio of the period of a structure to the thickness of a layer calculated according to the theoretical dependence (21), crosses represent values which are calculated from the wave number of the Fourier mode with the maximum amplitude. Mesh size 64×64.

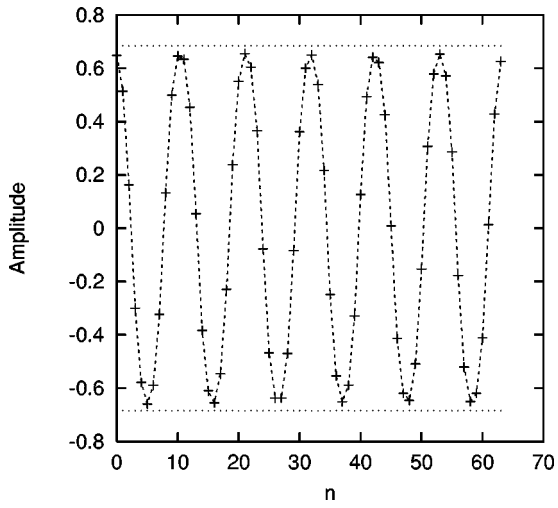

FIG. 5. The concentration dependence upon the coordinate oriented in the perpendicular direction to the plane of the rotating field. The cross section of the equilibrium pattern formed at h/l and $\mathrm{Bm}=0.8$ in the middle of the periodicity cell ($x=L_x/2$). Crosses represent the numerically calculated points, broken curve solely for server convenience, dotted line represents the values of the concentration amplitude calculated according to relation (20). Mesh size 64×64.

this action. An equilibrium distance between stripes is established due to the repulsion described by fifth term within the brackets under the Laplacian in Eq. (12) . The period and the amplitude of the concentration structure with stripes parallel to the plane of a rotating field in correspondence with a minimum of the thermodynamic potential can be calculated analytically. For the case of small layer thicknesses the corresponding relations are derived in Refs. [25,26]. The thermodynamic potential in an undimensional form for the case when a pattern is homogeneous in the plane of the rotating field yields the following form:

$$\Delta F+\Delta F_m = \frac{\alpha^2 h l^2}{\gamma}\left[\int\left(-\frac{1}{2}\varphi^2+\frac{1}{4}\varphi^4+\frac{1}{2}(\nabla\varphi)^2\right)dS + \frac{1}{2}\frac{\mathrm{Bm}}{(h/l)^2}\int\int J(\boldsymbol{\rho}-\boldsymbol{\rho}')\varphi(\boldsymbol{\rho})\varphi(\boldsymbol{\rho}')dSdS'\right]. \tag{14}$$

For the case of a periodic distribution of the concentration around a critical concentration value when

$$\varphi=\varphi(\boldsymbol{q})\cos(qx),$$

relation (14) for the volume density of the thermodynamic potential reads

$$\frac{\Delta F+\Delta F_m}{V}=\frac{\alpha^2}{4\gamma}\left[\left(q^2+\frac{\mathrm{Bm}}{(h/l)^2}J(q)-1\right)\varphi^2(\boldsymbol{q})+\frac{3}{8}\varphi^4(\boldsymbol{q})\right], \tag{15}$$

whereas relation (15) for the amplitude of the structure gives

$$\varphi^2(\boldsymbol{q})=\frac{4}{3}\left[1-\left(q^2+\frac{\mathrm{Bm}}{(h/l)^2}J(q)\right)\right]. \tag{16}$$

A period $2\pi/q$ for the stripe structure determined by a minimum of the thermodynamic potential (15) may be found from the relation

$$2q+\frac{\mathrm{Bm}}{(h/l)^2}J'(q)=0. \tag{17}$$

When $h\gg l$ $J\cong 2\pi/q$ and the wave number of an equilibrium stripe structure is determined by the following relation:

$$q=\left(\frac{\pi\mathrm{Bm}}{(h/l)^2}\right)^{1/3} \tag{18}$$

the amplitude of a structure reads

$$\varphi^2(\boldsymbol{q})=\frac{4}{3}\left[1-3\left(\frac{\pi\mathrm{Bm}}{(h/l)^2}\right)^{2/3}\right]$$

or if Bm_c is introduced as

$$\mathrm{Bm}_c=\frac{1}{3\sqrt{3}\pi}\left(\frac{h}{l}\right)^2, \tag{19}$$

the expression for the amplitude of the periodic pattern can be finally transformed into the following form:

$$\varphi^2(\boldsymbol{q})=\frac{4}{3}\left[1-\left(\frac{\mathrm{Bm}}{\mathrm{Bm}_c}\right)^{2/3}\right]. \tag{20}$$

Relation (19) for a critical value of the magnetic Bond number gives dependence of the critical value of the magnetic

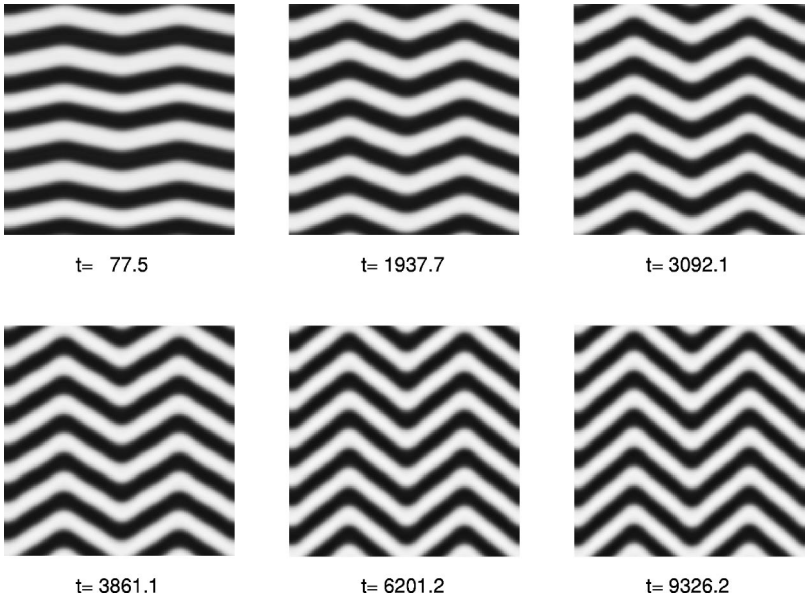

FIG. 6. Instability of a stripe pattern in the field normal to the boundaries of a Hele-Shaw cell. $h/l=5$. Initial state corresponds to the periodically disturbed final state obtained at Bm $=0.3$. Bm$=0.85$. Mesh size 64×64.

field strength upon the thickness of the plane layer obtained in Refs. [11,12] [$\beta=(\partial M/\partial n)^2 l_\star^2$]:

$$H-H_c=\left(\frac{3\sqrt{3\pi}l_\star}{h}\right)^{2/3}\frac{(\partial M/\partial n)^2}{\partial^2 M/\partial n^2}.$$

The results of numerical simulations are in fairly good agreement with a physical picture of the phenomena described above. Kinetics of formation of the stripe patterns upon the action of a rotating magnetic field for several values of the magnetic Bond number is shown in Figs. 1, 2, and 3, respectively. As one may see from Figs. 1–3 the patterns formed due to concentration fluctuation upon the action of a rotating field transform into the stripe structure which by typical coarsening process develops into a periodical system of stripes which run parallel to the plane of a rotating field. Merging and splitting of the stripes at intermediate stages lead to the formation of typical patterns with oblique stripes which are characteristic for the coarsening process mentioned above. An increase in the magnetic Bond number decreases the characteristic time of the structure formation and leads to the development of a finer pattern. The conclusions resulting from numerical calculations are in good agreement with conclusions from the theoretical model described above. Dependence of the period of a structure upon the magnetic Bond number obtained from the wave number corresponding to the Fourier mode of a concentration pattern with maximum amplitude is shown in Fig. 4. The broken line in Fig. 4 shows the dependence of a period of the pattern corresponding to a minimum of the thermodynamic potential (14) which in accordance with relation (18) equals

$$\frac{\lambda}{h}=\frac{2\pi}{[\pi\mathrm{Bm}(h/l)]^{1/3}}. \tag{21}$$

It is possible to conclude that the patterns formed upon the action of the rotating field reasonably well correspond to the energy minimum of a system consisting of parallel stripes. Small discrepancies could be due to kinetic peculiarities. This remark is especially relevant for the case Bm$=0.2$ since as one can see from Fig. 1 the state a system has reached after quite long pattern rearrangement process is not even strictly periodic due to a very slowly paced structure formation process. Obviously, this is related to the fact that the characteristic time of a structure rearangement process for small Bm is large enough and the system remains in a metastable state. In good agreement also are the values of the concentration modulation amplitudes as shown in Fig. 5 where concentration variation along a line in the perpendicular direction with respect to the plane of rotating field drawn in the middle of a periodicity cell is indicated for Bm$=0.8$ and $h/l=5$. The dotted lines indicate the theoretical values calculated from Eq. (20). The fact that during the structure rearrangement in a rotating magnetic field the state corresponding to the energetical minimum of a system of parallel stripes is achieved allows to predict several interesting phenomena. Since the period of a pattern formed upon the action of the rotating magnetic field diminishes with the increase in the magnetic Bond number as shown in Fig. 2 the pattern which is formed at lower values of the magnetic Bond number will be stretched for larger values. Then one can observe undulation instability leading to the formation of the chevron structure. The said occurrence is illustrated in Figs. 6, 7, and 8 for several magnetic Bond numbers Bm>0.3 where one can see the development of undulation deformations originating from the initial state, which corresponds to the final state reached at Bm$=0.3$. Initial distribution of the concentration corresponding to the periodic undulation deformation of a stripe pattern may be described as follows:

$$n'(x,y)=\begin{cases} n(x,y+\alpha x) & x\leqslant L_x/2, \\ n[x,y+\alpha(L_x-x)] & L_x/2<x<L_x, \end{cases}$$

where α is set equal to 0.2 in the present case. The way how characteristic chevron pattern from the initially imposed undulation deformations of the stripe structure develops is possible to observe in Fig. 6 (Bm$=0.85$,$h/l=5$). At larger values of the magnetic Bond number (Fig. 7, Bm$=1$,$h/l=5$, the final state at Bm$=0.3$ serves as initial state) the formation of the characteristic alternating finger pattern is ob-

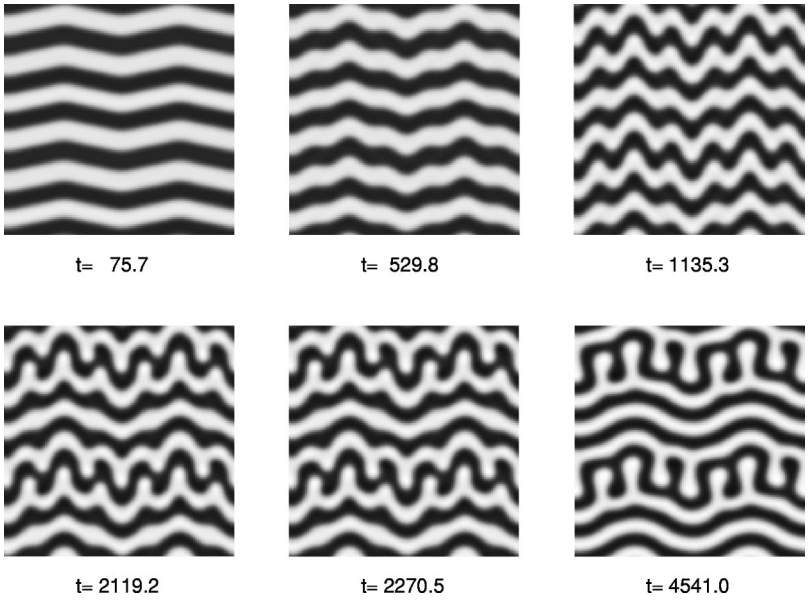

FIG. 7. The same as in Fig. 6 except for Bm $=1.0$.

served. Similar phenomena are also observed for macroscopic magnetic fluid stripes and may be related to the nonlinear supression of the overextension instability due to the vertex splitting [27] as corroborated by the results of the numerical simulation using the technique of boundary integral equations. As to the transformation of chevron patterns taking place at even higher values of the magnetic Bond number one can observe the onset of topological transformations connected with the merging and breaking of stripes (Fig. 8, Bm$=1.2$,$h/l=5$). It is interesting to remark that in the last case formation of the hairpins characteristic for the labyrinthine patterns in garnet films and ferrofluids could be also obtained [28]. Thus, the present model is sufficiently versatile in order to allow adequate simulation of the behavior of 2D systems in the presence of long-range dipolar forces. Also the present model might be used to study various instabilities within the chevron patterns [29]. There is an instability of the chevron pattern causing a split of the boundaries between the regions with homogeneous orientation of the stripes. A critical value of the angle between stripes $\pi-2\beta$ at a grain boundary can be calculated from the dependence of its energy on the angle between stripes at the grain boundary yielding the following equation [30]:

$$[\tan(\beta)]^{3/2}=\frac{2[\tan(\pi/4-\beta/2)]^{3/2}}{\sin(\pi/4+\beta/2)}.$$

In numerical experiments the instability of a grain boundary is induced by applying a stronger magnetic field to the structure formed at lower field. In this case the fingering at a grain boundary as was seen in Fig. 9 result in the formation of a characteristic pattern with hairpins which is also observed in garnet films and ferrofluids.

V. CONCLUSIONS

The proposed model for the formation of patterns in a Hele-Shaw cell upon the action of a rotating magnetic field on a phase separating magnetic fluid is in position to describe a wide variety of different phenomena. Upon the ac-

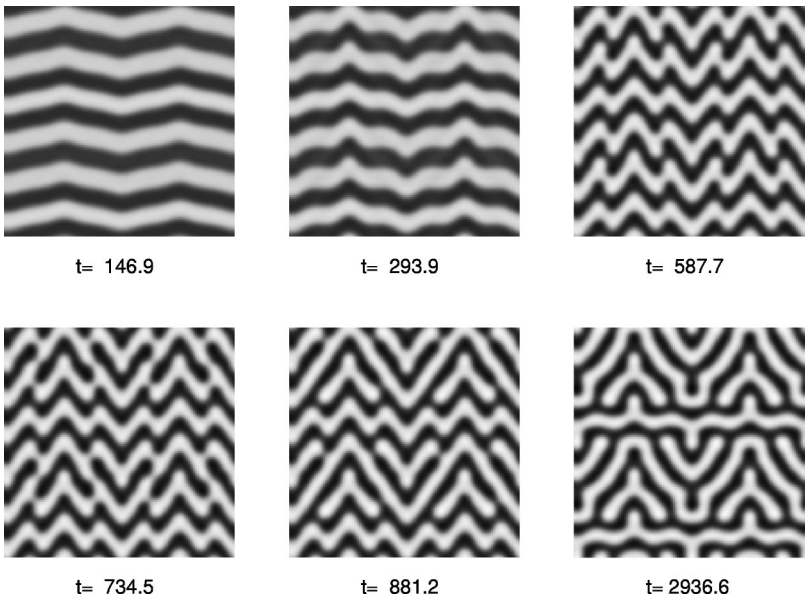

FIG. 8. The same as in Fig. 6, except for Bm$=1.2$.

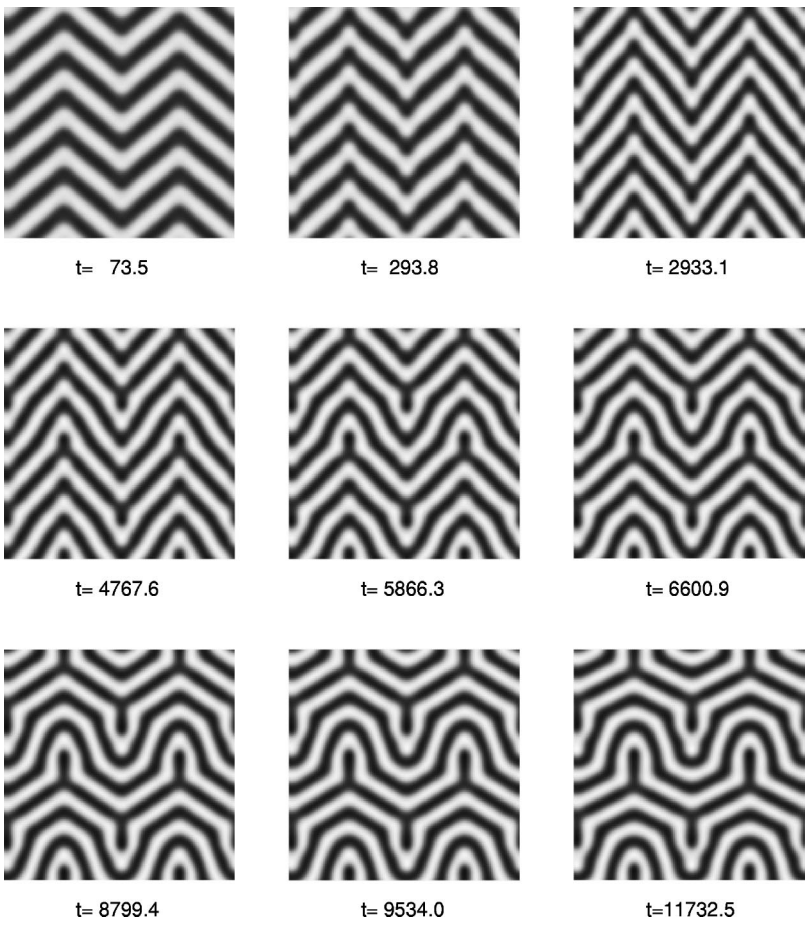

FIG. 9. The development of the instability of a grain boundary between the regions with homogeneous stripe orientation upon increasing the magnetic Bond number. $h/l=5$. The initial state corresponds to the equilibrium chevron pattern established at $\mathrm{Bm}=0.85$. Magnetic Bond number of a normal field applied to the chevron pattern equals $\mathrm{Bm}=1.2$.

tion of a rotating magnetic field the concentration nonhomogenities forming at the phase separation of a ferrocolloid, rearrange themselves into the stripes which undergo the characteristic coarsening process to develop a periodical pattern. During the rearrangement process merging and breaking of the stripes occur and characteristic pattern with oblique stripes finally transforms in a periodical system of the stripes parallel to the plane of a rotating magnetic field. The equilibrium distance between the stripes and the amplitude of the concentration modulation in an established structure corresponds quite well to the one calculated from the condition of an energy minimum. It is possible to induce different transformations of a stripe pattern by changing the value of the magnetic Bond number and eliminating component of a rotating field, which is orientated tangentially to the boundaries. Applying a magnetic field normal to the boundaries with the Bond number in excess of an initial value of the rotating field at which the stripe pattern has been created, one can observe a characteristic undulation instability leading to chevron structures; for higher values of the magnetic Bond number instabilities of undulating stripes leading to the structures with alternating fingers are observed. Breaking and merging of stripes during evolution of the undulation deformations at higher values of the magnetic Bond number are also a possibility. It is possible to induce instability of the boundaries between regions with homogeneous stripe orientation leading to the formation of the characteristic hairpin patterns by increasing the magnetic Bond number of a normal magnetic field applied to the formed chevron pattern.

[1] A. Cebers, Magni. Gidrodin. **2**, 42 (1982) [Magnetohydrodynamics **18**, 42 (1982)].
[2] K. Sano and M. Doi, J. Phys. Soc. Jpn. **52**, 2810 (1983).
[3] R. E. Rosensweig and J. Popplewell, in *Abstracts of the International Symposium on Electromagnetic Forces* (Sendai, Japan, 1991), p. 83.
[4] H. Zhang and M. Widom, J. Magn. Magn. Mater. **122**, 119 (1983).
[5] H. Zhang and M. Widom, Phys. Rev. E **49**, R3591 (1994).
[6] M. J. Stevens and G. S. Grest, Phys. Rev. Lett. **72**, 3686 (1994).
[7] M. J. Stevens and G. S. Grest, Phys. Rev. E **51**, 5962 (1995).
[8] M. J. Stevens and G. S. Grest, Phys. Rev. E **51**, 5976 (1995).
[9] D. Wei, Phys. Rev. E **49**, 2454 (1994).
[10] M. A. Osipov, P. I. C. Teixeira, and M. M. Telo da Gama, Phys. Rev. E **54**, 2597 (1996).
[11] A. Cebers, Magni. Gidrodin. **4**, 132 (1986) [Magnetohydrodynamics **24**, 132 (1988)].
[12] A. Cebers, Magni. Gidrodin. **2**, 57 (1988).
[13] Yu. A. Buyevich and A. Yu. Zubarev, J. Phys. II **3**, 1633 (1993).
[14] L. D. Landau and E. M. Lifshitz, Phys. Z. Sowjetunion **8**, 153 (1935).
[15] Th. C. Halsey, Phys. Rev. E **48**, R673 (1993).

[16] A. Cebers, Magni. Gidrodin. **31**, 61 (1995) [Magnetohydrodynamics **31**, 61 (1995)].
[17] C. Flament *et al.*, Europhys. Lett. **34**, 225 (1996).
[18] J. W. Cahn and J. E. Hilliard, J. Chem. Phys. **28**, 258 (1958).
[19] R. C. Desai, C. Sagui, and K. R. Elder, in *Structure and Dynamics of Strongly Interacting Colloids and Supramolecular Aggregates in Solution* (Kluwer Academic Publishers, Dordrecht, 1992), p. 205.
[20] C. Sagui and R. C. Desai, Phys. Rev. E **49**, 2225 (1994).
[21] A. Cebers, Magni. Gidrodi. **31**, 69 (1995) [Magnetohydrodynamics **31**, 69 (1995)].
[22] A. Cebers, Prog. Colloid Polym. Sci. **100**, 101 (1996).
[23] A. Cebers, J. Magn. Magn. Mater. **85**, 20 (1990).
[24] C. Canuto *et al.*, *Spectral Methods in Fluid Dynamics* (Springer Verlag, Berlin, 1988).
[25] D. Andelman, Fr. Brochard, and P. G. de Gennes, C. R. Acad. Sci., Ser. I: Math. **301**, 675 (1985).
[26] D. Andelman, Fr. Brochard, and J.-F. Joanny, J. Chem. Phys. **86**, 3673 (1987).
[27] A. Cebers and I. Drikis, Magni. Gidrodin. **32**, 11 (1996).
[28] M. Seul and R. Woffe, Phys. Rev. A **46**, 7534 (1992).
[29] A. C. Newell *et al.*, J. Phys. II **5**, 1863 (1995).
[30] A. Cebers and I. Drikis, in *Free Boundary Problems: Theory and Applications* (Chapman and Hall/CRC, London, 1999), p. 14.